

Ground-State Energy of Liquid He⁴†

M. A. Pokrant

University of Florida, Gainesville, Florida 32601

(Received 10 April 1972)

A compressibility-consistent integral equation for the radial distribution function g similar to a previously proposed pressure-consistent integral equation is applied to a $(b/r)^5$ effective potential. The results compare well with those obtained by a molecular-dynamics calculation and are superior to the results of Percus-Yevick 2 and Percus-Yevick 2 XS calculations. The g obtained from this integral equation can be used to compute the sum of the bridge diagrams. These bridge-diagram sums are used in an Euler-Lagrange equation to compute the ground-state Bijl-Jastrow wave function for liquid He⁴. An interatomic potential of the Lennard-Jones 6-12 type is used. The ground-state energy is found to be -6.63 °K/atom (experiment: -7.14 °K). The equilibrium density is 0.0205 atom/Å³ (experiment: 0.02185 atom/Å³). The structure factor and radial distribution function obtained are compared with experimental results.

I. INTRODUCTION

Several authors¹⁻¹¹ have made variational calculations to obtain the ground-state energy of liquid He⁴ assuming a Bijl-Jastrow-type trial wave function:

$$\psi = \exp\left[\frac{1}{2} \sum_{i < j} u(r_{ij})\right]. \quad (1.1)$$

This approximation allows the energy per atom to be written in terms of the radial distribution function as

$$E = T + V, \quad (1.2)$$

$$V = \frac{1}{2} \rho \int g(r) v(r) d\vec{r}, \quad (1.3)$$

$$T = -(\rho \hbar^2 / 8M) \int g(r) \nabla^2 u(r) d\vec{r}, \quad (1.4)$$

where

$$g(r) = N(N-1) \rho^{-2} \int \psi^* \psi d\vec{r}_3 \dots d\vec{r}_N / \int \psi^* \psi d\vec{r}_1 \dots d\vec{r}_N \quad (1.5)$$

and $v(r)$ is the interatomic potential, often taken to be the Lennard-Jones potential

$$v(r) = 4\epsilon[(\sigma/r)^{12} - (\sigma/r)^6] \quad (1.6)$$

with¹² $\epsilon = 10.22$ °K and $\sigma = 2.556$ Å.

Some authors¹⁻⁵ used a simple parametric form for u and obtained g by various methods. One advantage of varying u is that the relatively accurate Monte Carlo (MC) or molecular-dynamics (MD) methods may be used.¹⁻⁴ Because of the machine time needed, only a small number of parameters are feasible. Another drawback is that these methods cannot handle the long-range $1/r^2$ behavior predicted¹³⁻¹⁵ for u , but can only include it as a perturbation in an unsatisfactory manner.² The alternative of obtaining g from u by means of Born-Green, hypernetted-chain (HNC), Percus-Yevick (PY), or other integral equations avoids

the latter drawback and largely alleviates the former. Unfortunately, these are approximate equations which sometimes give poor results.

Another approach⁶⁻⁸ is to vary g and use an approximate relation to obtain u . A considerable advantage is that if the PY or HNC approximation is used, then u may be obtained from g by a direct calculation instead of the iteration procedures necessary to obtain g from u . The machine time thus saved may be used to consider more complicated parametric forms. If the Born-Green equation is used,⁶⁻⁸ an iterative process is still necessary, but the machine time needed is far less than that required for a MC or MD calculation. The primary disadvantage of varying g is the uncertainty in the u because of approximations made in deriving the integral equation. Another drawback is that g has more structure than u and more parameters are needed to obtain a good approximation to the function. Also, g must be restricted to those functions which can be generated by a boson wave function by forcing g to satisfy various necessary conditions.¹⁶⁻¹⁹ The problem of determining sufficient conditions has not been solved.

The best approach is to consider the variation of E when $u(r)$ is allowed to vary arbitrarily and solve the resulting Euler-Lagrange equation. Campbell and Feenberg (CF) have done this⁹⁻¹¹ using the HNC and PY approximations. The method employed in this paper is an attempt to solve the Euler-Lagrange equation by using an approximation superior to the HNC or PY approximations.

II. DERIVATION OF EULER-LAGRANGE EQUATION

In this section the variational principle will be used to derive an integral equation for the radial distribution function for liquid He⁴. This equation will be an extension of the one previously derived by CF. Their notation will be used as much as

possible. From Eqs. (1.2)–(1.4) the energy is

$$E = \frac{1}{2}\rho \int g(r) V^*(r) d\vec{r} \quad (2.1)$$

where

$$V^*(r) = v(r) - \frac{1}{2} \alpha \nabla^2 u(r), \quad \alpha = \hbar^2/2M. \quad (2.2)$$

The variational principle states that the best energy will be obtained when

$$\frac{\delta E}{\delta u(\vec{r})} = 0. \quad (2.3)$$

With the use of Eq. (2.1) this condition becomes²⁰

$$\frac{1}{2} \alpha \nabla^2 g(r) = \int V^*(r') \frac{\delta g(\vec{r}')}{\delta u(\vec{r})} d\vec{r}'. \quad (2.4)$$

The methods of classical statistical mechanics which were developed to obtain the radial distribution function give us a relationship between g and u ²¹:

$$g(r) = e^{N(r)+B(r)+u(r)}, \quad (2.5)$$

where N and B are the sums of the nodal and bridge diagrams, respectively. $N(r)$ can be expressed as a function of the structure factor

$$\tilde{N} = (S-1)^2/\rho S, \quad S = 1 + \rho \tilde{G}, \quad (2.6)$$

where the tilde denotes the Fourier transform and $G = g - 1$. Multiplying Eq. (2.2) by g and eliminating u with the aid of Eq. (2.5), we obtain

$$gV^*(r) = gv + \frac{1}{2} \alpha (\nabla g \cdot \nabla g/g + g\nabla^2 B + G\nabla^2 N - \nabla^2 C), \quad (2.7)$$

where

$$C(r) = G(r) - N(r), \quad \tilde{C} = (S-1)/\rho S.$$

To obtain the quantity on the right-hand side of Eq. (2.4), start by taking the functional derivative of Eq. (2.5). With the use of Eq. (2.6) this gives

$$\frac{\delta g(\vec{r})}{\delta u(\vec{r}')} = g(r) \left[\delta(\vec{r} - \vec{r}') + \int e^{i\vec{k} \cdot (\vec{r} - \vec{r}')} \left(\frac{S^2(k) - 1}{S^2(k)} \right) \times \frac{\delta g(\vec{r}'')}{\delta u(\vec{r}')} d\vec{r}'' + \frac{d\tilde{C}}{(2\pi)^2} + \frac{\delta B(\vec{r})}{\delta u(\vec{r}')} \right]. \quad (2.8)$$

In this investigation, the last term will be neglected; this is equivalent to using the HNC functional derivative. $B(r)$ will be assumed to be a function which does not change when $u(r)$ changes; this is not equivalent to the HNC approximation unless $B(r) = 0$. Even with this simplification, the resulting integral equation cannot be solved analytically and would be extremely difficult to solve on a computer. However, as suggested by CF, we define a new function

$$Q(r) = \int V^*(r') \frac{\delta g(\vec{r})}{\delta u(\vec{r}')} d\vec{r}'. \quad (2.9)$$

This will be useful only if the right-hand side of

Eq. (2.4) can be replaced by $Q(r)$. This will be the case only if the functional derivative is symmetric in \vec{r} and \vec{r}' . Both the exact functional derivative and the HNC approximation to it have this property¹¹; the PY approximation does not.

To obtain an equation for $Q(r)$, multiply Eq. (2.8) by $V^*(r')$ and integrate over $d\vec{r}'$. Identify a factor $Q(r')$ inside the integrals on the right-hand side of the resulting equation. The use of Fourier transforms then reduces the equation to

$$Q(r) = g(r) V^*(r) + g(r) [(S^2 - 1) \tilde{Q}/S^2]^F, \quad (2.10)$$

where the superscript F denotes the Fourier transform. This equation may be rearranged to give

$$(\tilde{Q}/S^2)^F = gV^* + G[(S^2 - 1) \tilde{Q}/S^2]^F. \quad (2.11)$$

In order to obtain a form which may be easily solved numerically, we define

$$\tilde{L}(k) = \rho \tilde{Q}(k)/S^2(k) \quad (2.12)$$

and

$$V_k^* = (\rho g V^*)^F. \quad (2.13)$$

These definitions allow Eq. (2.11) to be rewritten

$$\tilde{L}(k) = V_k^* + \{G[(S^2 - 1) \tilde{L}]^F\}^F, \quad (2.14)$$

which is the same as Eq. (71) of CF.¹⁰

Now, the minimization condition, Eq. (2.4), in terms of Q is

$$Q(r) = \frac{1}{2} \alpha \nabla^2 g(r) \quad (2.15)$$

or, equivalently, using the definition in Eq. (2.12),

$$\tilde{L}(k) = -\frac{1}{2} \alpha k^2 (S-1)/S^2. \quad (2.16)$$

The problem is now reduced to solving Eqs. (2.14) and (2.16) simultaneously using the definitions in Eqs. (2.7) and (2.13) plus some approximation for $\nabla^2 B(r)$. If we set $\nabla^2 B(r) = 0$, then these equations are equivalent to those obtained by CF.

The procedure for obtaining a solution is to guess an S and obtain L by solving Eq. (2.14) by iteration using Eq. (2.16) as an initial guess. Then we use CF's suggestion for the new trial function

$$\hat{S} = S/(S + 2LS^2/\alpha k^2)^{1/2} \quad (2.17)$$

and repeat the entire procedure until successive structure factors are equal to the desired degree of accuracy.

One may also combine Eqs. (2.7), (2.14), and (2.16) to obtain a single equation rather than two coupled equations:

$$\frac{2}{\alpha} gv + 2G\nabla^2 g + \frac{\nabla g \cdot \nabla g}{g} + g \left(\frac{k^2(S^2 - 1)}{\rho S^2} \right)^F + g\nabla^2 B = 0. \quad (2.18)$$

Except for the last term, this is the same as CF's Eq. (82) (which should have a factor of g on the right-hand side).

TABLE I. Comparison of kinetic, potential, and total energies (in °K/atom) obtained by molecular dynamics and compressibility-consistent method for $u = -(1.17\sigma/r)^5$.

ρ/ρ_0	Schiff and Verlet ^a			Compressibility-consistent method			
	T	V	E	T	V	E	m
0.90	11.87	-17.79	-5.92	11.80	-17.76	-5.96	-0.161
0.95	12.95	-18.81	-5.86	12.89	-18.84	-5.95	-0.152
1.00	14.10	-19.78	-5.68	14.01	-19.89	-5.88	-0.143

^aData computed from Table I in Ref. 2.

It is interesting to note that the same equation could have been derived by setting

$$\frac{\delta E}{\delta g(\vec{r})} = 0. \quad (2.19)$$

This can be seen in CF's Eq. (85) or by setting

$$\frac{\delta B(\vec{r})}{\delta u(\vec{r}')} = 0 \quad (2.20)$$

in Eq. (13) of Lee and Broyles.²⁰ This is a consequence of the fact that we have employed an approximation which provides a direct relationship between g and u , and which leads to a functional derivative of $g(\vec{r})$ with respect to $u(\vec{r}')$ which is symmetric in \vec{r} and \vec{r}' .

III. METHOD FOR OBTAINING $B(r)$

It would be desirable to obtain $\nabla^2 B(r)$ from a relatively accurate calculation, i. e., a MD or MC calculation. We will consider the MD calculation of Schiff and Verlet.² They used

$$u(r) = -(b\sigma/r)^5 \quad (3.1)$$

and determined that $b = 1.17$ gave the best energy at the experimental density of liquid He⁴, $\rho_0 = 0.02185$ atom/Å³. Since $g(r)$ is tabulated, one can use Eqs. (2.5) and (2.6) to determine $B(r)$. Unfortunately, the data points are not smooth enough to obtain a useful $\nabla^2 B$.

Carley and Lado²² and Rowlinson²³ have suggested the approximation

$$B(r) = m(ge^{-u} - 1 - \ln ge^{-u}), \quad (3.2)$$

where m is a parameter to be determined. The HNC approximation is given by $m = 0$, while $m = 1$ yields the PY approximation. Rowlinson²³ and Lado²⁴ further suggested that the condition of pressure consistency be used to determine m . Calculations using this and slightly different procedures have given mixed results.²⁵ We will use the similar method of compressibility consistency.

The idea behind introducing the pair approximation to the wave function in Eq. (1.1) is to regard u as an effective classical potential divided by kT so that the methods of classical statistical

mechanics can be used to calculate g . Therefore, m will be determined by requiring that the derivative of the classical pressure divided by kT with respect to the density obtained from the virial relation

$$\frac{\partial \beta P}{\partial \rho} = \frac{\partial}{\partial \rho} \left(\rho + \frac{1}{6} \rho^2 \int_0^\infty r g(r) u'(r) 4\pi r^2 dr \right) \quad (3.3)$$

be equal to the same quantity obtained from the compressibility relation

$$\frac{\partial \beta P}{\partial \rho} = 1 - \rho \int_0^\infty C(r) 4\pi r^2 dr. \quad (3.4)$$

These compressibility-consistent equations are easier to solve than the pressure-consistent method which requires integrating Eq. (3.4) over the density starting from a reference density at which the pressure is known.

The calculation was done for the $u(r)$ given by Eq. (3.1) with b fixed at 1.17. To obtain a solution, we guessed m , computed g , calculated the pressure from the virial relation for three densities, and took the numerical derivative of the pressure. The results of Eqs. (3.3) and (3.4) were then compared. This was repeated until an m was found for which the two quantities differed by less than 0.1%. This procedure determined m with an estimated error of $\pm 2\%$. The method of calculating the derivative of the pressure with respect to the density was checked on a sample calculation by varying the density increment and by using five densities instead of three. $B(r)$ was then obtained from Eq. (3.2). This calculation was repeated for each density considered. The energies are compared with those obtained by Schiff and Verlet in Table I. Tables II and III compare $g(r)$ and $S(k)$ at $\rho = \rho_0$. The energies calculated by this method may be seen to be clearly superior to results of Percus-Yevick 2 and Percus-Yevick 2 XS⁵ methods by comparing the numbers in Table I with Figs. 1 and 10 of Ref. 5.

IV. METHOD OF CALCULATION

In solving Eqs. (2.14) and (2.16) simultaneously, a problem arises in calculating the improved radial distribution function \hat{g} . The straightforward method would be to simply calculate it from \hat{S} . However, it is impossible to obtain sufficient numerical accuracy to have \hat{g} vanish at the origin properly. CF suggested using a different method of calculating \hat{g} . Their method is equivalent to using Lado's perturbation formula,²⁶ in which the bridge diagrams are assumed to remain unchanged,

$$\hat{g} = g e^{\hat{N} - N + \hat{u} - u}, \quad (4.1)$$

and the change in u is approximated by

$$\hat{u} - u = \hat{C} - C, \quad (4.2)$$

where \hat{N} and \hat{C} are defined in terms of \hat{S} . Then

$$\hat{g} = g e^{U(\hat{S}-S)/\rho} \quad (4.3)$$

Now, if g vanishes properly, so will \hat{g} . Although the two methods of calculating \hat{g} differ only at small r , an additional problem has now arisen in that \hat{g} and \hat{S} are no longer completely consistent. There are several terms in Eqs. (2.7) and (2.14) which may be written as functions of either g or S . CF used \hat{g} in Eq. (2.7) and \hat{S} in Eq. (2.14). We have used \hat{g} in those places where g or G is shown explicitly and \hat{S} everywhere else; i. e., \hat{S} has been used wherever possible and \hat{g} has been used when it appears that its small- r properties might be important.

For an initial guess, we used the S obtained in Sec. III with some alterations to obtain linear be-

TABLE II. Comparison of radial distribution functions of Schiff and Verlet (SV) with compressibility-consistent (cc) result at $\rho = \rho_0$; $m = -0.143$, $b = 1.17$.

r/σ	g_{sv}	g_{cc}	r/σ	g_{sv}	g_{cc}
≤ 0.72	0	0	2.24	0.976	0.976
0.76	0.002	0.001	2.28	0.985	0.982
0.80	0.010	0.009	2.32	0.986	0.988
0.84	0.037	0.036	2.36	0.987	0.994
0.88	0.099	0.097	2.40	0.992	0.999
0.92	0.209	0.201	2.44	1.003	1.003
0.96	0.347	0.347	2.48	1.008	1.006
1.00	0.512	0.517	2.52	1.009	1.009
1.04	0.680	0.694	2.56	1.010	1.010
1.08	0.841	0.859	2.60	1.012	1.011
1.12	0.976	0.999	2.64	1.012	1.012
1.16	1.095	1.109	2.68	1.013	1.012
1.20	1.174	1.188	2.72	1.012	1.011
1.24	1.232	1.237	2.76	1.011	1.010
1.28	1.255	1.262	2.80	1.010	1.009
1.32	1.268	1.268	2.84	1.010	1.007
1.36	1.264	1.259	2.88	1.007	1.006
1.40	1.251	1.240	2.92	1.006	1.004
1.44	1.233	1.214	2.96	1.004	1.003
1.48	1.206	1.184	3.00	1.003	1.002
1.52	1.162	1.153	3.04	1.001	1.001
1.56	1.129	1.122	3.08	1.000	1.000
1.60	1.099	1.092	3.12		0.999
1.64	1.069	1.065	3.16		0.998
1.68	1.041	1.040	3.20		0.998
1.72	1.020	1.018	3.24		0.997
1.76	1.004	0.999	3.28		0.997
1.80	0.986	0.983	3.32		0.997
1.84	0.975	0.970	3.36		0.997
1.88	0.966	0.961	3.40		0.997
1.92	0.955	0.955	3.44		0.998
1.96	0.953	0.951	3.48		0.998
2.00	0.950	0.950	3.52		0.998
2.04	0.948	0.951	3.56		0.999
2.08	0.950	0.954	3.60		0.999
2.12	0.952	0.958	3.64		0.999
2.16	0.953	0.964	3.68		1.000
2.20	0.961	0.970			

TABLE III. Comparison of structure factor of Schiff and Verlet with compressibility-consistent result at $\rho = \rho_0$; $m = -0.143$, $b = 1.17$.

$k\sigma$	S_{sv}	S_{cc}	$k\sigma$	S_{sv}	S_{cc}
0.0		0.083	8.7	0.950	0.948
0.3	0.085	0.086	9.0	0.958	0.955
0.6	0.094	0.093	9.3	0.968	0.964
0.9	0.105	0.103	9.6	0.978	0.975
1.2	0.120	0.117	9.9	0.988	0.985
1.5	0.135	0.135	10.2	1.000	0.995
1.8	0.157	0.159	10.5	1.008	1.004
2.1	0.186	0.189	10.8	1.012	1.010
2.4	0.224	0.229	11.1	1.014	1.014
2.7	0.275	0.281	11.4	1.013	1.016
3.0	0.345	0.349	11.7	1.012	1.016
3.3	0.430	0.437	12.0	1.011	1.015
3.6	0.540	0.547	12.3	1.008	1.013
3.9	0.680	0.680	12.6	1.006	1.010
4.2	0.840	0.830	12.9	1.003	1.007
4.5	0.980	0.980	13.2	1.001	1.003
4.8	1.115	1.108	13.5	1.000	1.001
5.1	1.201	1.192	13.8		0.998
5.4	1.236	1.226	14.1		0.996
5.7	1.219	1.217	14.4		0.995
6.0	1.174	1.180	14.7		0.995
6.3	1.122	1.132	15.0		0.995
6.6	1.075	1.083	15.3		0.995
6.9	1.031	1.039	15.6		0.996
7.2	1.001	1.003	15.9		0.997
7.5	0.975	0.977	16.2		0.998
7.8	0.956	0.959	16.5		0.999
8.1	0.948	0.949	16.8		1.000
8.4	0.946	0.946			

havior at the origin. The variational calculation was first performed neglecting the bridge diagrams and then repeated using the results of the previous section for $\nabla^2 B$. Eqs. (2.14) and (2.16) were iterated until S_{rms} defined by

$$S_{rms} = \left\{ \sum_{i=1}^N [\hat{S}(k_i) - S(k_i)]^2 \Delta k_i \right\}^{1/2} \quad (4.4)$$

was less than 10^{-4} . About seven iterations were usually necessary. Sixteen significant figures were carried throughout the calculations. Up to 1024 points were employed. The adequacy of the range in r was checked by varying the range while holding the increment constant and comparing various quantities, including the energy. Results of a typical calculation are illustrated in Fig. 1. Figure 2 shows the change when the increment was varied while the range was fixed.

V. RESULTS

We first solved Eqs. (2.14) and (2.16) in the HNC approximation ($B=0$) in order to compare with CF's result. CF computed the energy in several different ways at the experimental density.

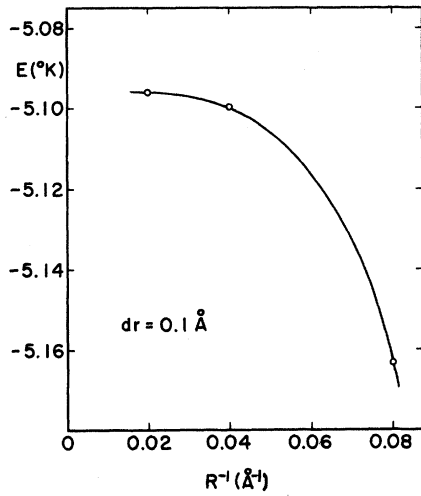


FIG. 1. Energy as a function of inverse range R^{-1} for a fixed increment dr .

First, their paired-phonon analysis predicted a perturbation of the energy due to the change of the structure factor from their initial guess (-0.73 °K). They added this to the starting energy calculated by Massey and Woo⁸ using the Kirkwood superposition approximation in the Bogoliubov-Born-Green-Kirkwood-Yvon (BBGKY) equation (-5.97 °K) to obtain a total energy of -6.70 °K. CF evidently considered this to be their primary result. When they calculated the energy directly from their final structure factor using the Kirkwood superposition and the BBGKY equation, an energy of -5.91 °K was obtained. This discrepancy is due to the fact that the optimization procedure minimizes the HNC energy rather than the

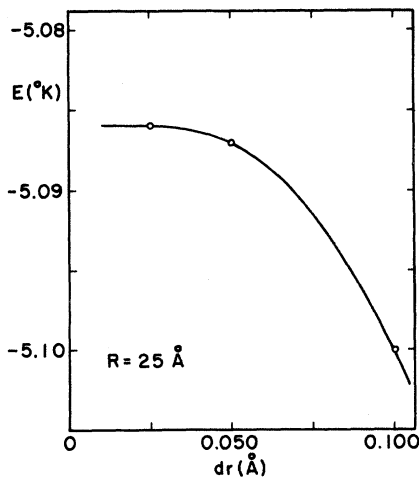


FIG. 2. Energy as a function of increment dr for a fixed range R .

TABLE IV. Comparison of energies (in °K/atom) and speed of sound (in m/sec) in the HNC approximation.

	T	V	E	c
Campbell and Feenberg	16.64	-20.69	-4.04	219
Present calculation (HNC)	14.80	-19.89	-5.09	183

Massey-Woo energy. CF also calculated both the starting energy and the final energy directly, using only the HNC approximation, and obtained -3.40 and -4.04 °K, respectively. The energy shift is in reasonable agreement with that predicted by their perturbation calculation. Since we used only the HNC approximation, we should compare with the final result of CF which contains only the HNC approximation (-4.04 °K). As illustrated in Table IV and Fig. 3 the energies disagree by more than 1 °K. The structure factors and radial distribution functions differed by a small but significant amount. This must be due either to a numerical error or the different use of the inconsistent \hat{g} and \hat{S} in the various parts of the calculation. Use of different starting functions might also cause a discrepancy because of the inconsistency of \hat{g} and \hat{S} . It would seem that the initial guess with the lowest energy should be preferred.

Support for the validity of the present calculation is obtained from a comparison with a calcula-

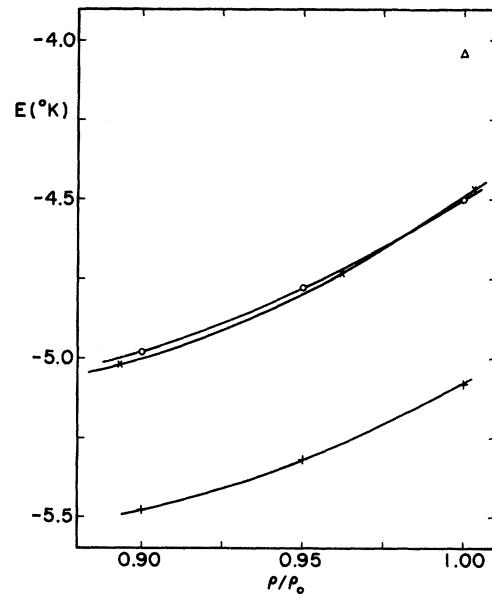


FIG. 3. Ground-state energy of liquid He^4 as a function of density in the HNC approximation: triangle, Campbell and Feenberg (Ref. 10); crosses, Murphy and Watts (Ref. 3); circles, initial guess for present calculation; plus signs, final result for present calculation in the HNC approximation.

TABLE V. Energies (in °K/atom) and speed of sound (in m/sec) obtained by variational method when the sum of the bridge diagrams is included as a fixed function.

ρ/ρ_0	T	V	E	c
0.90	11.27	-17.85	-6.58	99
0.93	11.87	-18.50	-6.63	118
0.95	12.28	-18.91	-6.63	130
1.00	13.36	-19.96	-6.60	160

tion by Murphy and Watts³ shown in Fig. 3. They applied the HNC approximation to the effective potential $u = -(b/r)^5$ and varied b to find the minimum in the energy. Since their energy lies below CF's energy, the CF energy cannot very well be optimized. The PY results given in Refs. 3 and 10 show a similar disagreement. From the similarity of the form of the variational function used by Murphy and Watts to the form used in Sec. III and its relation to our initial guess function, one would expect our initial energy to be comparable to the energy calculated by Murphy and Watts. One would not necessarily expect the energies to be identical because the calculation in Sec. III included an approximation to the bridge diagrams and did not minimize the HNC energy. Also, the results were altered to obtain a linear structure factor at the origin. Actually, the energies are nearly equal as illustrated in Fig. 3. The minimization procedure then lowers the energy by about 0.5 °K from the initial energy, which is not an unreasonable amount.

The primary result of this investigation was the solution of Eqs. (2.14) and (2.16) with the approximation to the sum of the bridge diagrams included

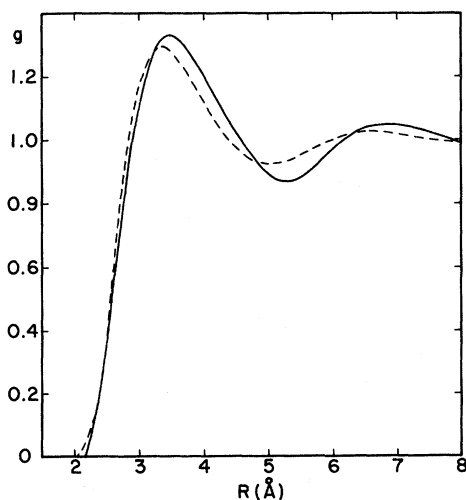


FIG. 4. Radial distribution function of liquid He⁴ ($\rho = \rho_0$): solid line, x-ray scattering at 0.79 °K (Ref. 29); dashed line, present calculation.

in the calculation. This calculation gave a considerably lower energy than that obtained when the HNC approximation was employed. Table V lists the speed of sound and energies obtained at four densities. The speed of sound was computed by combining the relation

$$S \rightarrow \hbar k / 2Mc \text{ as } k \rightarrow 0 \quad (5.1)$$

with Eqs. (2.14) and (2.16) to obtain¹¹

$$\begin{aligned} Mc^2 &= \tilde{L}(0) \\ &= 2E - \frac{\hbar^2}{4M} \int G(r) \left[\int e^{i\vec{k}\cdot\vec{r}} [S(k) - 1] \right. \\ &\quad \left. \times \left(1 - \frac{1}{S^2(k)} \right) k^2 \frac{d\vec{k}}{(2\pi)^3} \right] d\vec{r}. \end{aligned} \quad (5.2)$$

While the energies are closer to experiment than any of the MC or MD calculations,¹⁻⁴ the speed of sound is quite poor compared to the experimental value of 238 m/sec at $\rho = \rho_0$. This disappointing result is evidently due to having neglected the variation of the bridge diagrams and to the sensitivity of the calculation of the speed of sound to the behavior of the structure factor at all values of k as shown by Eq. (5.2). The speed of sound may also be computed by differentiating the energy-density curve:

$$P = \rho^2 \frac{\partial E}{\partial \rho}, \quad (5.3)$$

$$Mc^2 = \frac{\partial P}{\partial \rho} = \frac{\partial}{\partial \rho} \left(\rho^2 \frac{\partial E}{\partial \rho} \right). \quad (5.4)$$

If the four points in Table V are used to fit the energy as a function of density using a quadratic least-squares fit, the speed of sound at $\rho = \rho_0$ is found to be 258 m/sec. However, since only four points were used and there is an uncertainty of one in the third significant figure in the energy, the second derivative of the energy with respect to the density cannot be very accurate, and the above quantity, therefore, has considerable uncertainty. The energy at $\rho = \rho_0$ is -6.60 °K, in rough agreement with CF's primary result of -6.70 °K. The two procedures are

TABLE VI. Comparison of equilibrium density and energy obtained by various methods.

Author	ρ_{eq}/ρ_0	E (°K/atom)
McMillan	0.89 ± 0.01	-5.9 ± 0.1
Schiff and Verlet	0.9 ± 0.1	-5.95 ± 0.2
Murphy and Watts	0.89	-5.96
Murphy ^a	0.92	-5.93
Pokrant	0.94	-6.63
Expt.	1.00	-7.14

^aWithout three-body energy.

TABLE VII. Radial distribution function of liquid He⁴ when the approximation to the bridge diagrams is included at $\rho = \rho_0$.

$R(\text{\AA})$	g	$R(\text{\AA})$	g
≤ 1.841	0	4.805	0.933
1.943	0.001	4.908	0.927
2.045	0.009	5.010	0.925
2.147	0.037	5.112	0.926
2.249	0.099	5.214	0.930
2.352	0.206	5.316	0.936
2.454	0.353	5.419	0.944
2.556	0.525	5.521	0.953
2.658	0.703	5.623	0.964
2.760	0.870	5.725	0.974
2.863	1.014	5.828	0.984
2.965	1.125	5.930	0.994
3.067	1.207	6.032	1.002
3.169	1.260	6.134	1.010
3.272	1.287	6.237	1.016
3.374	1.293	6.339	1.020
3.476	1.283	6.441	1.023
3.578	1.262	6.543	1.024
3.681	1.233	6.646	1.024
3.783	1.199	6.748	1.023
3.885	1.162	6.850	1.021
3.987	1.124	6.952	1.019
4.090	1.087	7.055	1.016
4.192	1.054	7.157	1.012
4.294	1.023	7.259	1.009
4.396	0.996	7.361	1.005
4.499	0.974	7.464	1.002
4.601	0.956	7.566	0.999
4.703	0.942		

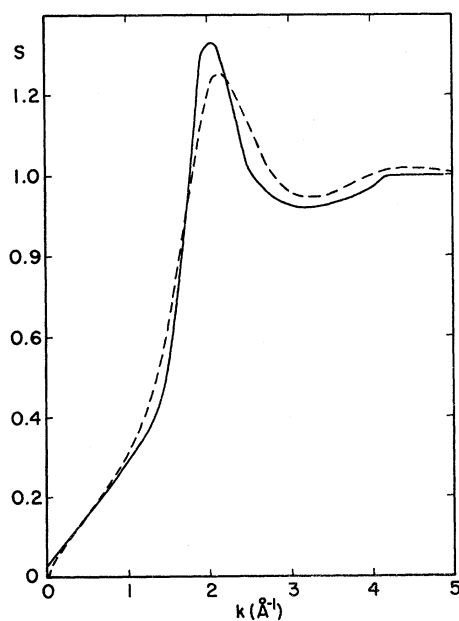


FIG. 5. Structure factor of liquid He⁴ ($\rho = \rho_0$): solid line, x-ray scattering at 0.79°K (Ref. 29); dashed line, present calculation.

not directly comparable, however, since CF used Massey and Woo's value for the initial energy and used the HNC approximation to minimize the energy and compute the energy shift. On the other hand, we have included the approximation to the bridge diagrams both in the minimization procedure and in the calculation of the energy. Table VI compares the energy and equilibrium density computed here with the quantities calculated by other authors using MC or MD methods and a parametrized $u(r)$. The contribution of the triple-dipole three-body interaction to the energy²⁷ has been removed from Murphy's tabulated results⁴ to make all of the energies comparable. Inclusion of the triple-dipole three-body interaction would raise all of the energies slightly and lower the equilibrium density by a small amount. Since other many-body terms are neglected and there is considerable uncertainty in the Lennard-Jones potential, this alteration is only a small part of the total error. Tables VII and VIII list the radial distribution function and the structure factor, respectively, at the experimental density.

The structure factor of liquid He⁴ has been measured by x-ray scattering²⁸⁻³¹ and by neutron scattering³² at various temperatures. The lowest tem-

TABLE VIII. Structure factor of liquid He⁴ when the approximation to the bridge diagrams is included at $\rho = \rho_0$.

$k (\text{\AA}^{-1})$	S	$k (\text{\AA}^{-1})$	S
0	0	3.24	0.945
0.12	0.056	3.36	0.947
0.24	0.098	3.48	0.953
0.36	0.130	3.60	0.962
0.48	0.158	3.72	0.973
0.60	0.186	3.84	0.984
0.72	0.216	3.96	0.995
0.84	0.251	4.08	1.004
0.96	0.291	4.20	1.011
1.08	0.340	4.32	1.015
1.20	0.400	4.44	1.016
1.32	0.476	4.56	1.016
1.44	0.571	4.68	1.015
1.56	0.689	4.80	1.012
1.68	0.832	4.92	1.009
1.80	0.991	5.04	1.006
1.92	1.140	5.16	1.003
2.04	1.236	5.28	1.000
2.16	1.260	5.40	0.998
2.28	1.226	5.52	0.996
2.40	1.167	5.64	0.995
2.52	1.105	5.76	0.995
2.64	1.052	6.00	0.996
2.76	1.010	6.24	0.997
2.88	0.980	6.48	0.999
3.00	0.960	6.72	1.000
3.12	0.949		

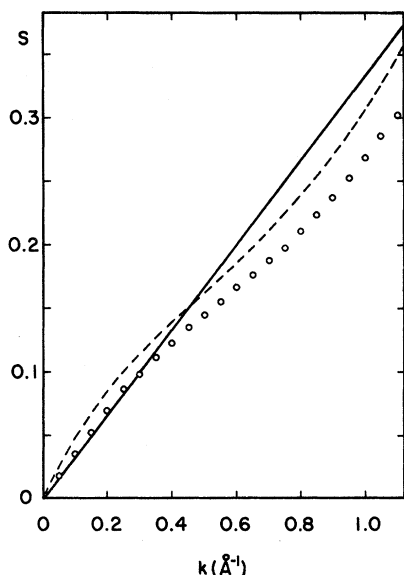


FIG. 6. Small k structure factor of liquid He⁴ ($\rho = \rho_0$): solid line, Feynman prediction; circles, x-ray scattering (Ref. 31); dashed line, present calculation.

perature studied where a large range of k was covered was 0.79 °K by Achter and Meyer.²⁹ The $g(r)$ and $S(k)$ determined by the variational method are compared with their results in Figs. 4 and 5. As is characteristic of most theoretical calculations done to date, the peaks and valleys of both g and S show rather poor agreement with experiment. However, the various experimental results at different temperatures also vary considerably. Hallock^{30,31} has recently measured $S(k)$ for small k at a temperature of 0.38 °K. Our results are compared with his smoothed results extrapolated to 0 °K in Fig. 6.

VI. CONCLUSIONS

The compressibility-consistent method for computing radial distribution functions was found to give very good agreement with the MD calculations for a $1/r^5$ effective potential in the particular case studied. In addition, the bridge diagrams from this calculation can be used to significantly improve variational calculations of the ground-state energy. If we allow arbitrary variations of the wave functions, as opposed to single-parameter variations, the discrepancy between theoretical and experimental determinations of the energy is approximately halved.

It has been noted by other authors^{2-4,7,11} that altering the constants in the Lennard-Jones potential or replacing it by other reasonable potentials can give drastically different results for the energies. Hence, use of a superior potential might yield far better agreement with experiment. Unfortunately, other potentials which have been proposed have too much uncertainty to be very useful at this time.⁴

There are several obvious ways in which the present calculation could be improved. One way would be to calculate the $u(r)$ from the final result, and use it to solve the compressibility-consistent integral equation for a new $B(r)$. Then solve the Euler-Lagrange equation and iterate. A better method might be to approximate $\delta B(\vec{r})/\delta u(\vec{r}')$ in Eq. (2.8) using Eq. (3.2) as a guide.

ACKNOWLEDGMENTS

The author is indebted to Professor A. A. Broyles for many helpful suggestions and critical comments on the manuscript. He also thanks F. A. Stevens, Jr., for interesting discussions. He would also like to thank Professor E. Feenberg, Dr. C. E. Campbell, and Dr. Tucson Dunn, each of whom sent unpublished material which was helpful.

†Work supported in part by a grant from the National Science Foundation.

¹W. L. McMillan, Phys. Rev. **138**, A442 (1965).

²D. Schiff and L. Verlet, Phys. Rev. **160**, 208 (1967).

³R. D. Murphy and R. O. Watts, J. Low Temp. Phys. **2**, 507 (1970).

⁴R. D. Murphy, Phys. Rev. A **5**, 331 (1972).

⁵W. P. Francis, G. V. Chester, and L. Reatto, Phys. Rev. A **1**, 86 (1970).

⁶W. E. Massey, Phys. Rev. Letters **12**, 719 (1964).

⁷W. E. Massey, Phys. Rev. **151**, 153 (1966).

⁸W. E. Massey and C. W. Woo, Phys. Rev. **164**, 256 (1967).

⁹C. E. Campbell, doctoral dissertation (Washington University, 1968) (unpublished).

¹⁰C. E. Campbell and E. Feenberg, Phys. Rev. **188**, 396 (1969).

¹¹E. Feenberg, *Theory of Quantum Fluids* (Academic, New York, 1969).

¹²J. DeBoer and A. Michels, Physica **5**, 945 (1938).

¹³R. P. Feynman, Phys. Rev. **94**, 262 (1954).

¹⁴J. E. Enderby, T. Gaskell, and N. H. March, Proc. Phys. Soc. (London) **85**, 217 (1965).

¹⁵L. Reatto and G. V. Chester, Phys. Rev. Letters **22**, 276 (1966).

¹⁶M. Yamada, Progr. Theoret. Phys. (Kyoto) **25**, 579 (1961).

¹⁷C. Garrod and J. K. Percus, J. Math. Phys. **5**, 1756 (1964).

¹⁸E. Feenberg, J. Math. Phys. **6**, 658 (1965).

¹⁹F. Y. Wu, H. T. Tan, and E. Feenberg, J. Math. Phys. **8**, 864 (1967).

²⁰J. C. Lee and A. A. Broyles, Phys. Rev. Letters **17**, 424 (1966).

²¹E. E. Salpeter, Ann. Phys. (N. Y.) **5**, 183 (1958); A. Münster, *Statistical Thermodynamics* (Academic, New York, 1969), Vol. 1, p. 636ff.

²²D. D. Carley and F. Lado, Phys. Rev. **137**, A42

(1965).

²³J. S. Rowlinson, *Mol. Phys.* **9**, 217 (1965).²⁴F. Lado, *J. Chem. Phys.* **47**, 4828 (1967).²⁵F. Mandel and R. J. Bearman, *J. Chem. Phys.* **55**, 4762 (1971), and references therein.²⁶F. Lado, *Phys. Rev.* **135**, A1013 (1964).²⁷R. D. Murphy and J. A. Barker, *Phys. Rev. A* **3**, 1037 (1971).²⁸W. Gordon, C. S. Shaw, and J. Daunt, *J. Phys. Chem. Solids* **5**, 117 (1958).²⁹E. K. Achter and L. Meyer, *Phys. Rev.* **188**, 291 (1969); *Phys. Rev. A* **4**, 811(E) (1971).³⁰R. B. Hallock, *Phys. Rev. Letters* **23**, 830 (1969).³¹R. B. Hallock, *Phys. Rev. A* **5**, 320 (1972).³²D. G. Henshaw, *Phys. Rev.* **119**, 9 (1960).

PHYSICAL REVIEW A

VOLUME 6, NUMBER 4

OCTOBER 1972

Application of the Equation-of-Motion Method to the Spectrum of Superfluid Helium. I

Charles P. Enz*

IBM Zurich Research Laboratory, 8803 Rüschlikon, Switzerland

(Received 25 June 1971; revised manuscript received 15 November 1971)

The two three-body correlation terms occurring in the equation of motion for the density response function are expressed in terms of three-point vertex functions. By neglecting retardation effects in the latter, this leads to frequency-dependent effective kinetic and potential energies $K_{\text{eff}}(\vec{q}, \omega)$ and $V_{\text{eff}}(\vec{q}, \omega)$. K_{eff} is expressed by the one-particle correlation functions and V_{eff} by the density correlation function. K_{eff} and V_{eff} determine the density response function $\chi(\vec{q}, \omega)$, the poles of which define the phonon-roton spectrum ω_q . In addition, an eigenvalue equation is derived which is shown to have two distinct eigenvalues. While the first is again ω_q , the second is identified with the diffuse second branch recently found by Cowley and Woods. It is shown that in the limit $q \rightarrow \infty$ the two eigenvalues both merge into the free-particle spectrum. The limit $q \rightarrow 0$ of the two eigenvalues as well as the end-point singularity of the phonon-roton branch are discussed in a second paper.

I. INTRODUCTION

The latest very detailed neutron-scattering results of Cowley and Woods¹ for superfluid He⁴ clearly show that the excitation spectrum consists of two branches, the well-known sharp phonon-roton branch and a very diffuse branch at about twice the energy of the latter, which at wave numbers $q \geq 3 \text{ \AA}^{-1}$ oscillates slightly below the free-particle energy $\epsilon_q = \hbar^2 q^2 / 2m$ (see Figs. 6 and 21 of Ref. 1). While it was already well known that at large q the spectrum follows the free-particle excitation curve² this second branch has not before been followed down into the q region of the phonon-roton branch (see, however, Ref. 3).

Another striking feature established in Ref. 1 but known already from earlier results of the same authors³ is the flattening of the phonon-roton branch at twice the roton gap, and its sudden disappearance at $q \approx 3.5 \text{ \AA}^{-1}$. This behavior is an impressive confirmation of a prediction made by Pitaevskii.⁴

In this and a subsequent paper⁵ we propose to analyze the features mentioned as well as the behavior of the two branches in the long-wavelength limit from an atomic point of view. This task is essentially the same as that of the recent work of

Iwamoto⁶ who, starting from the atomic Hamiltonian, first eliminates the condensate variables by a canonical transformation and then applies a Bogoliubov transformation. His approximation consists in a Tamm-Dancoff cutoff of states containing more than two Bogoliubov quasiparticles. Not surprisingly this leads to a two-branch spectrum which, for separable interactions, is argued to have the qualitative features of the spectrum found by Cowley and Woods. Of course, a higher-order Tamm-Dancoff cutoff would lead to more than two branches, and the question may be asked whether further experiments should not be expected to reveal such higher branches, too.

Our analysis is based on the equation of motion for the density response function. Similar equation-of-motion techniques have been previously applied to superfluid helium by Eters⁷ and by Tserkovnikov.⁸ Both these works are generalized random-phase approximations (RPA) in the sense that they apply RPA to certain generalized density operators. In this way Eters obtained a generalization of the Bogoliubov approximation and calculated the temperature dependence of the sound velocity. Taking two essentially canonically conjugate densities, Tserkovnikov obtained two poles of the corresponding Green's functions which in the long-wavelength limit describe first